ADVANCED MATERIALS
www.advmat.de

www.MaterialsViews.com

Large-Scale Colloidal Synthesis of Non-Stoichiometric $Cu_2ZnSnSe_4$ Nanocrystals for Thermoelectric Applications

*Feng-Jia Fan, Yi-Xiu Wang, Xiao-Jing Liu, Liang Wu, and Shu-Hong Yu**

Due to the important applications in refrigeration and waste heat to electricity conversion, thermoelectric (TE) materials have drawn considerable attention among materials researchers.[1] TE modules outperform conventional mechanical electricity generators and air-conditioners in simplicity and long-term reliability, but the relatively low efficiencies of current TE modules limit their large-scale commercialization.[2] The performance of TE materials is quantified by the TE figure of merit ZT ($ZT = \sigma S^2 T/\kappa$), where σ, S, T, and κ are the electric conductivity, the Seebeck coefficient, the absolute temperature, and the thermal conductivity, respectively. During the past two decades, remarkable enhancements in thermoelectric properties have been obtained in nanostructured bulk materials.[3] There are two typical successful methods of introducing nanostructures into bulk thermoelectric materials leading to improved TE properties: ball milling of element ingots and subsequent hot-pressing has been used in preparing $Bi_xSb_{2-x}Te_3$[1c,4] and $Si_{20}Ge_{80}$[5] nanostructured bulk materials, and thermal processing of appropriate material to form nanoscale precipitates in the bulk matrix has been applied to prepare PbSnTe/PbS,[6] PbS/PbTe,[7] and $PbNa_xTe$/SrTe[8] nanocomposites. Most bulk nanostructured TE materials with enhanced figure of merits benefit from depressed thermal conductivities, but enhancements in their power-factors have also been achieved.[8]

Wet-chemistry synthesis of thermoelectric nanoparticles and then compacting them into dense materials with extensive nanocrystalline boundaries provides another efficient approach to depress thermal conductivities. The feasibilities in nanoparticle size and morphology controls make the compacted materials hold promise to meet the requirements of the quantum-confinement effect; thus, enhanced thermoelectric properties could be expected.[9] Recently, there have been increasing reports based on wet-chemistry synthesis of thermoelectric nanoparticles, such as Bi_2Te_3,[10] $Bi_xSb_{2-x}Te_3$,[11] $Bi_2Te_xSe_{3-x}$,[12] Cu_2ZnSnS_4,[13] $Cu_2CdSnSe_4$,[14] $Cu_2ZnGeSe_4$,[15] and $Ag_2S_xSe_{1-x}$[16] nanoparticles; the TE properties of the compacted dense materials have also been reported, but there are few reports showing significant improvements of the TE properties.[10c,11b] Off-stoichiometry[14] and residue of insulated organic ligands in the dense materials[10b] are two possible reasons for the deterioration of the TE properties of compacted materials; furthermore, low outputs, typically ranging from several tens to several hundreds of milligrams, hinder the optimization of the parameters in subsequent compacting or annealing procedures might be another possible reason. Sometimes, one bulk material was made out of nanocrystals collected from several or dozens of batches,[14] and the possible variations in chemical composition or size of nanocrystals obtained from different batches would have an uncertain impact on the final TE properties. Most importantly, the ability to scale up is pivotal for the final applications of TE materials. Up to now, however, there have been few reports on solution-based synthesis of nanoparticles yielding over gram-scale products for TE applications after a single one-pot reaction.[10c,17] Furthermore, $Cu_2ZnSnSe_4$ (CZTSe) and its analogs,[18] such as $Cu_2CdSnSe_4$[18a,19] and Cu_2SnSe_3 (CTSe),[20] have attracted intensive attention due to their reasonably good TE properties after being doped; however, the TE properties of dense CZTSe-based material made from the colloidal nanocrystals have not been reported yet.

Herein, we demonstrate a wet-chemical approach for the large-scale colloidal synthesis of thermoelectric non-stoichiometric CZTSe nanocrystals yielding 10 g of product per run. The obtained CZTSe nanocrystals were hot-pressed into dense materials and the effect of different hot-pressing temperatures on the TE properties of the dense materials was also explored. The peak ZT value of the compacted materials reaches 0.44 at 450 °C, which is similar to the state-of-the-art ZT values of CZTSe- and CTSe-based materials at similar temperatures. In principle, the synthetic procedure here is highly extendable; therefore, other binary, ternary, or quaternary selenide nanocrystals could be possibly prepared through similar procedures.

Non-stoichiometric CZTSe nanocrystals were prepared through a high-temperature colloidal-solution procedure with oleylamine (OLA) and 1-octadecene (1-ODE) as reaction mediums. To get over 10 g of product after one single reaction, large reaction flasks were used, and precursors with high concentrations were involved in the reaction. SeO_2 rather than Se powder was used as the selenium source, as it is much easier to be dissolved than Se powder and can be reduced to elemental Se by OLA or 1-ODE at elevated temperature. Elemental Se can be easily dissolved in trioctylphosphine (TOP), but TOP itself is very sensitive to oxygen and need to be handled in a glovebox, which is not favorable for a large-scale synthesis. Diorgano diselenide (di-*tert*-butyl diselenide or diphenyl diselenide), which can be easily dissolved in oleylamine, has also been used as a selenium source for synthesizing ternary and quaternary selenide nanocrystals;[21] however, the yielded product crystallizing in metastable wurtzite-derived phases would transform

Dr. F.-J. Fan, Y.-X. Wang, X.-J. Liu, L. Wu, Prof. S. H. Yu
Division of Nanomaterials and Chemistry
Hefei National Laboratory for Physical Sciences at the Microscale
Department of Chemistry
the National Synchrotron Radiation Laboratory
University of Science and Technology of China, Hefei
Anhui 230026, P.R. China
E-mail: shyu@ustc.edu.cn

DOI: 10.1002/adma.201202860

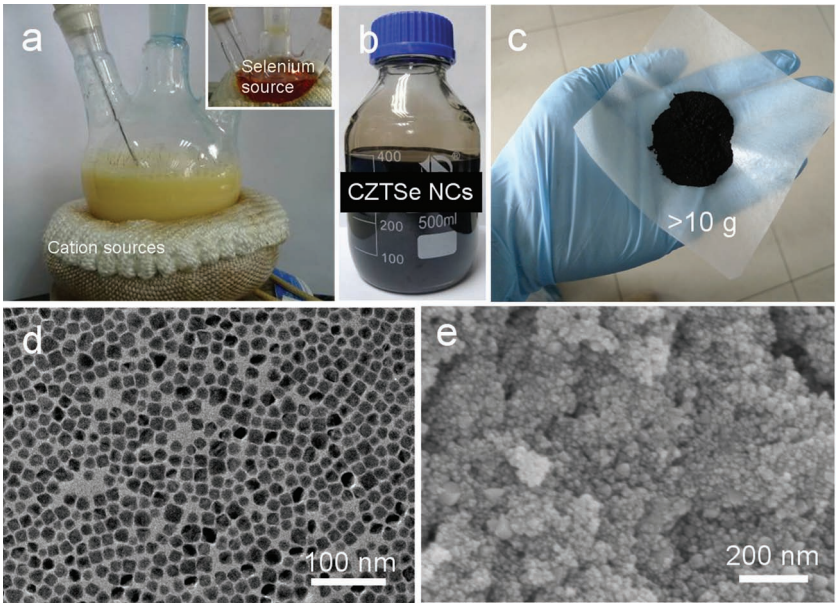

Figure 1. a–c) Photographs of the reaction flasks (a), the obtained non-stoichiometric CZTSe nanocrystals dispersed in hexane (b), and the surface-clean non-stoichiometric CZTSe nanoparticles (c). d,e) TEM (d) and SEM (e) images of the non-stoichiometric CZTSe nanoparticles.

during the hot-pressing process and measurements of the TE properties.

Figure 1a shows the two reaction flasks: the bigger one with the capacity of 250 mL contains metal cation precursors dissolved in 200 mL of OLA, and the 50 mL flask contains SeO_2/1-ODE solution. The reaction was started through adding SeO_2/1-ODE solution into the metal salts solution. After reaction, the nanocrystals were washed with hexane and ethanol. The obtained nanocrystals can be well dispersed in non-polar solvents, such as hexane, toluene, and chloroform, to form stable, dark-brown dispersions. The photograph in Figure 1b shows the dense dispersion of non-stoichiometric CZTSe nanocrystals in 400 mL of hexane with a concentration of about 25 mg mL^{-1}. UV–vis–near IR (NIR) spectrum of the nanocrystals dispersed in hexane indicates they have strong absorbance among the visible region (Supporting Information, Figure S1); thus, this is why the nanocrystal dispersion is brown colored. The size distribution and morphology of the synthesized nanocrystals were characterized by transmission electronic microscopy (TEM). The obtained nanocrystals, with an average diameter of 25 nm, are nearly monodisperse, and most of the nanoparticles display cube-like morphologies (Figure 1d). Before the hot-pressing procedure, a two-phase ligand-exchange procedure modified from previous reports was applied[10a] to remove the organic capping-ligands. The photographic (Figure 1c) and SEM images (Figure 1e) show the surface-clean nanoparticles, the yield of the surface-clean nanocrystals after one single reaction is more than 10 g. The average chemical composition of the obtained nanocrystals, which was determined by inductively coupled plasma (ICP) analysis, can be described as $Cu_2Zn_{0.03}Sn_{1.10}Se_{2.98}$, indicating that the Zn sources show much-lower reactivity than the Cu and Sn sources, as has been found in previously reported synthesis of CZTSe and Cu_2ZnSnS_4 nanocrystals.[22]

Powder X-ray diffraction (PXRD) was applied to characterize the crystal structure of the obtained nanocrystals. Considering that Zn content is very low in the obtained nanocrystals, and the molar ratio of Cu:Sn:Se is close to 2:1:3, the obtained non-stoichiometric CZTSe nanocrystals can be expected to accommodate the crystal structure of Cu_2SnSe_3 rather than that of kesterite or stannite CZTSe. In a previous report, Cu_2SnSe_3 was found to crystallize at room temperature in a monoclinic structure with the unit-cell parameters $\beta = 109.19°$, $a = 6.967$ Å, $b = 12.0493$ Å, and $c = 6.9453$ Å.[23] This structure can be taken as the derivative of the zinc-blende structure (**Figure 2** shows the unit cell of monoclinic Cu_2SnSe_3): a selenium atom is located at the center of a slightly distorted tetrahedron, of which the corners are occupied by (3 Cu atoms + one Sn atom) or (2 Cu atoms + 2 Sn atoms). The Cu–Se bond network offers a conductive matrix and the diversity in bonding types makes Cu_2SnSe_3 display a relatively low lattice thermal conductivity.[20] Figure 2b shows a PXRD pattern of the prepared non-stoichiometric CZTSe nanocrystals, which shows good agreement with the literature data.[23]

To characterize the TE properties of compacted bulk materials made from non-stoichiometric CZTSe nanocrystals, 1.8 g of surface-clean nanoparticles were hot-pressed into dense pellets under the same uniaxial pressure of 60 MPa at 350, 450, and 550 °C for 0.5 h. It can be seen from the inset photographs in **Figure 3**a that the dense pellet hot-pressed at 350 °C doesn't have a metallic luster, but those pellets hot-pressed at 450 and 550 °C display an obvious metallic sheen (insets in Figure 3b and 3c). The scanning electronic microscopy (SEM) images of the fracture surfaces of the compacted pellets are shown in Figure 3. We can observe that the coalescence and regrowth of nanocrystals are obvious after hot-pressing at even 350 °C; the

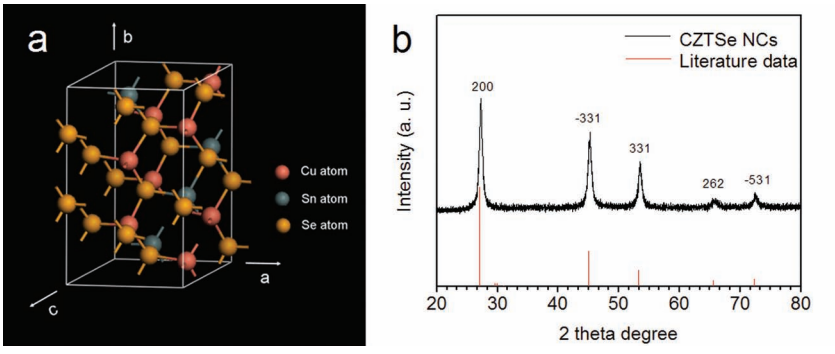

Figure 2. a) Unit cell of monoclinic CTSe. b) PXRD pattern of the prepared non-stoichiometric CZTSe nanocrystals and the literature data of CTSe.

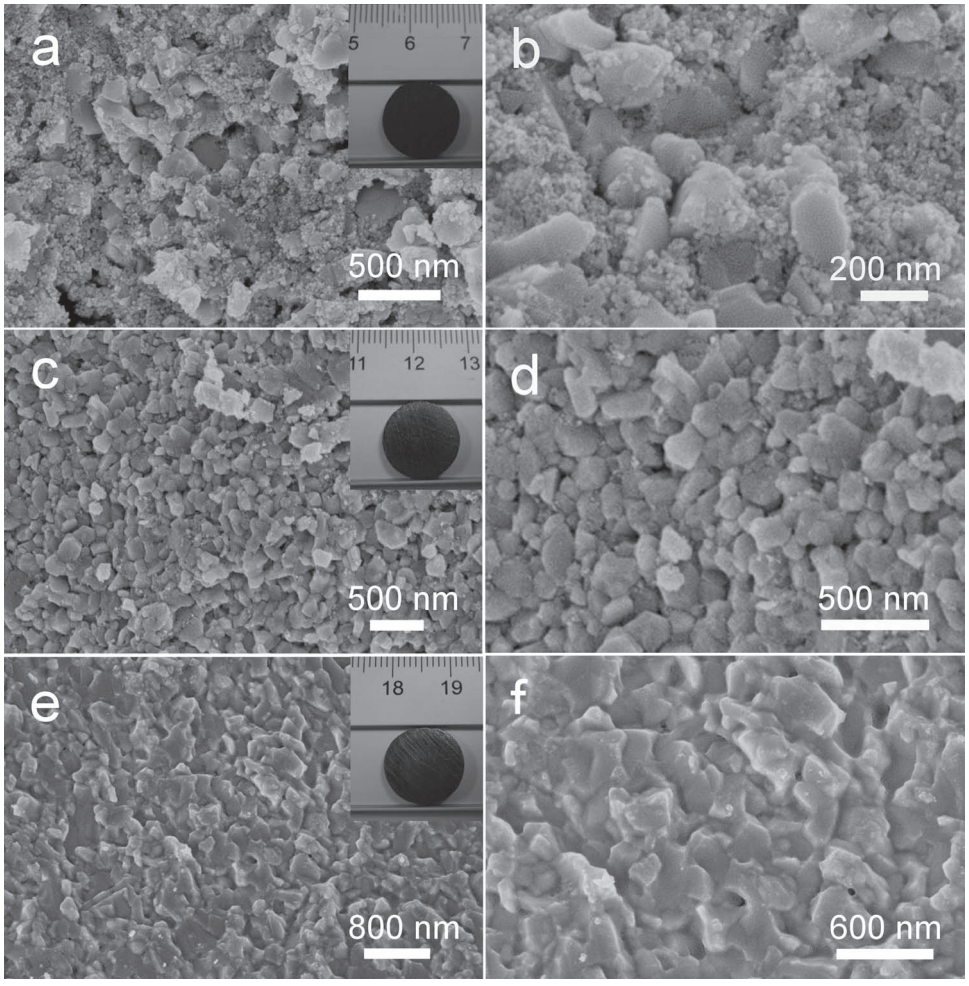

Figure 3. SEM images of the fracture surfaces of bulk materials compacted from non-stoichiometric CZTSe nanoparticle at different hot-pressing temperatures: a,b) 350 °C; c,d) 450 °C; e,f) 550 °C. The insets show photographs of the hot-pressed pellets.

size of some of the coalesced nanoparticles can be up to about 200 nm, but there are still a number of nanoparticles remaining almost the original sizes. When the hot-pressing temperature is increased to 450 °C, almost all of the small nanocrystals coalesce and regrow to form larger nanoparticles, with sizes ranging from several tens to several hundreds of nanometers. After hot-pressing at 550 °C, the size of the large nanoparticles further increases to around 500 nm. Reasonably, from the SEM images, we observed that the voids of the hot-pressed pellets decease as the hot-press temperature increases, leading to the increase in density from 5.1 to 5.6 g cm^{-3} (determined by the Archimedes' method). We also found that all of the pellets do not show noticeable anisotropic texture, as we found in $Cu_2CdSnSe_4$ nanostructured pellets.[14] The densities of all of the hot-pressed samples are no less than 85% of the theory value, and all of the pellets are mechanically robust enough to endure the dicing and polishing process. For the pellets hot-pressed at higher temperatures, they show stronger mechanical properties, which are favorable for practical thermoelectric applications. The regrowth and coalescence of the nanocrystals can be further confirmed through the X-ray diffraction (XRD) analysis, where we find the full width half maxima (FWHM) of the diffraction peaks are much narrower than the original nanocrystals (Supporting Information, Figure S2).

Bar samples with dimensions about 1.5 mm × 1.5 mm × 10 mm were diced from the disk samples for measuring the electric conductivities and Seebeck coefficients perpendicular to the press directions. As **Figure 4**a shows, the electric conductivities of the three samples fall in the ranges of 25 000–29 000 S m^{-1} and 18 000–24 000 S m^{-1} at room temperature and 450 °C, respectively, which are larger than those of previously reported undoped CZTSe[18] and CTSe[20] at the given temperatures. The enhancements in the electric conductivities can be attributed to the selenium vacancies in the compacted bulk materials, which increase the hole concentrations.[14] At room temperature, the sample hot-pressed at 550 °C shows a larger electric conductivity than the one hot-pressed at 350 °C, but the latter sample shows a higher electric conductivity measuring at a temperature above 150 °C; a clear reason for the different temperature dependence is not clear at the present stage. For the Seebeck coefficients, a larger sample density leads to a higher value within the measured temperature range, and the Seebeck coefficients increase with temperature monotonously (Figure 4b). The Seebeck coefficients of the three samples reach

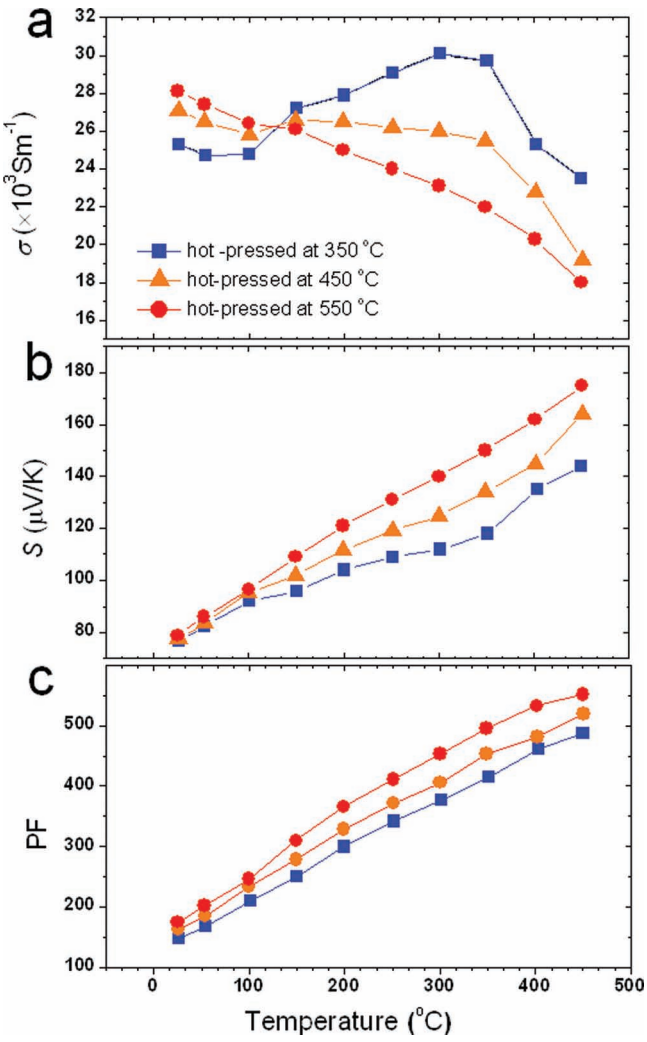

Figure 4. Temperature dependence of: a) electric conductivity (σ), b) Seebeck coefficient (*S*), c) power factor (*PF*) of the compacted bulk materials, for different hot-pressing temperatures.

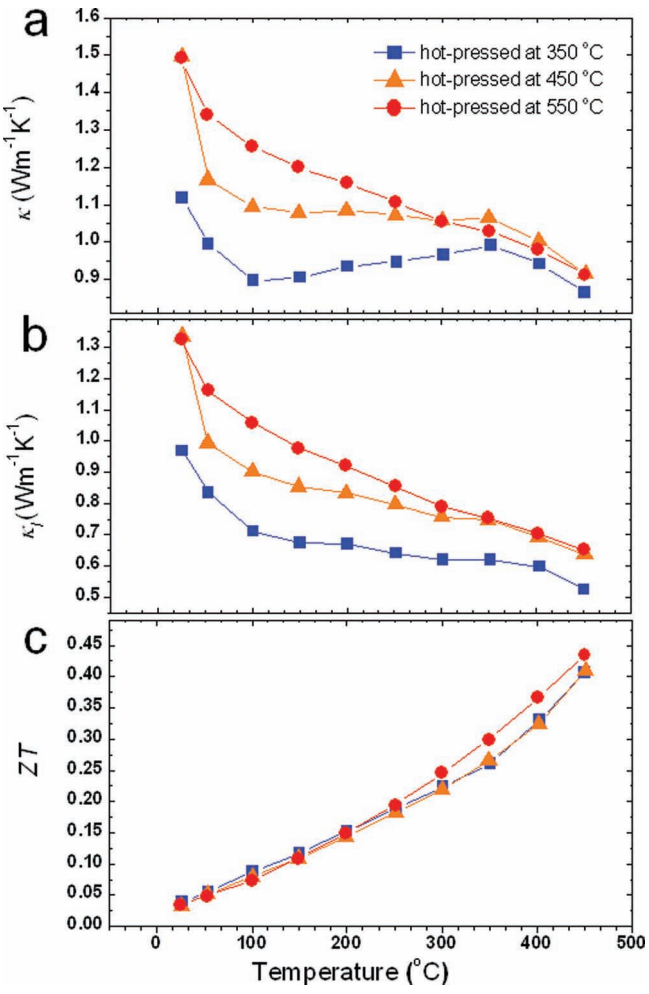

Figure 5. Temperature dependence of: a) thermal conductivity (κ); b) lattice thermal conductivities (κ_L); and c) *ZT*.

the peak values of 144, 164, and 175 μV K^{-1} at 450 °C, which are lower than those of undoped CZTSe and CTSe bulk and are comparable to those of the doped CZTSe and CTSe.[18,20] We calculated the power-factors ($PF = \sigma S^2$) and found that they are proportional to the densities of samples at the fixed measuring temperatures and increase monotonously with the temperature (Figure 4c). The peak power-factor of the sample hot-pressed at 550 °C is 0.55 mW m^{-1} K^{-2} (observed at 450 °C) and it is likely to increase further at elevated temperatures.

Disk samples with thicknesses around 1 mm and diameters around 12.5 mm were used to characterize the thermal conductivity (κ) parallel to the press direction. As illuminated in **Figure 5**a, our compacted materials show thermal conductivities that range from 1.1 to 1.5 W m^{-1} K^{-1} at room temperature, and all of the three samples display the lowest thermal conductivity at 450 °C, which varies from 0.87 to 0.91 W m^{-1} K^{-1}. The thermal conductivities of our samples are much smaller than the values reported previously for CZTSe and CTSe (both around 2.8 W m^{-1} K^{-1} at room temperature and 1.1 W m^{-1} K^{-1} at 450 °C) within the measured temperatures ranges;[18,20] this can be understood by enhanced phonon scattering at the point defects and the numerous crystalline boundaries. To make a comparison of the lattice thermal conductivities between our compacted pellets and those of previously reported bulk materials,[18b] we calculated the lattice thermal conductivities based on $\kappa_L = \kappa - \kappa_e$, where the electronic contribution κ_e is estimated based on the Wiedemann–Franz law ($\kappa_e = L_o \sigma T$, L_o = 2.0×10^{-8} W Ω K^{-2} (Supporting Information, Figure S3)). The lattice thermal conductivities of all our samples are more than 40% and 30% lower than those of the undoped CZTSe bulk materials at room temperature and 427 °C,[18b] respectively (Figure 5b). For the compacted pellet hot-pressed at 350 °C, the lattice thermal conductivities can be low: about 33% and 50% of the values of the undoped CZTSe bulk materials at room temperature and 427 °C,[18b] respectively.

We calculated the temperature dependence of *ZT* values by using the electric conductivities and Seebeck coefficients measured perpendicular to the press direction and the thermal conductivities parallel to the press direction, since our previous research has found that $Cu_2CdSnSe_4$, an analog of CZTSe, shows highly anisotropic transport properties.[14] We found that

the obtained pellets also do not show noticeable anisotropic texture as we found in $Cu_2CdSnSe_4$ nanostructured cylinders (Figure 3). The *ZT* values of the three samples show similar temperature dependences and are close to each other, indicating the final *ZT* values of the pellets show weak correlation with the hot-press temperature, or even the individual transport properties varies with the hot-press temperature (Figure 5c). The *ZT* values increase with temperature rising from room temperature to 450 °C, and the peak *ZT* value reaches 0.44, which is similar to the-state-of-the-art value of CZTSe- and CTSe-based semiconductors.[18,20] Compared with the previously reported[18,20] solid reaction synthesis of CZTSe- and CTSe-based materials, the synthesis temperature of our procedure (280 °C) is much lower, and the reaction time is highly shortened (30 min); thus, the synthetic method developed here will compete well in energy saving.

To conclude, we demonstrate an up-scaled colloidal synthesis of selenide nanocrystals yielding more than 10 g of product after one single reaction for thermoelectric applications. The obtained non-stoichiometric CZTSe nanocrystals were hot-pressed into dense materials at different temperatures; due to the increased crystalline boundaries, all of the samples show depressed thermal conductivities compared with previously reported CZTSe or CTSe bulk materials.[18,20] The final *ZT* values of all of the samples show similar temperature dependence and are similar to each other; the peak *ZT* value of 0.44 is comparable to the state-of-the-art value of CZTSe- and CTSe-based materials at a similar temperature.[18,20] Proper doping would possibly lead to a better thermoelectric performance. Even scale-up synthesis of thermoelectric nanocrystals is critical to further research and applications of solution-processed thermoelectric materials. This is the first example demonstrating that over 10 g of thermoelectric nanocrystals can be prepared by a single one-pot solution-based reaction, and this is also the first report on the thermoelectric properties of dense CZTSe-based materials made out of colloidal nanocrystals.

Experimental Section

Chemicals: Ethanol (99.7%), hexane (97%), $N_2H_4{\cdot}H_2O$ (85%), CuCl (97%), $Zn(CH_3COO)_2{\cdot}2H_2O$ (99%), $SnCl_2{\cdot}2H_2O$ (98%), and SeO_2 (99.0%) were purchased from Sinopharm Chemical Reagent Co. Ltd (Shanghai). Oleylamine (OLA) (80%-90%) and 1-octadecene (1-ODE, 90%) were purchased from Aladdin Reagent Co. Ltd (Shanghai). All of the chemical reagents were used as received without further purification.

Synthetic Procedure: To prepare non-stoichiometric CZTSe nanocrystals, we dissolved 10 g of SeO_2 in 50 mL of 1-ODE at 80 °C under vacuum for more than 6 h till a clear orange color solution formed. 4.5 g of CuCl, 5.1 g of $Zn(CH_3COO)_2{\cdot}2H_2O$, and 5.1 g of $SnCl_2{\cdot}2H_2O$ were mixed in 200 mL of oleylamine in another three-necked flask; the mixture was pumped for 6 h at room temperature to remove water, and then slowly heated to 180 °C (5 °C min^{-1}) and held at this temperature for 10 min under vacuum to get a bright yellow dispersion. The dispersion was subsequently cooled to 100 °C. The former SeO_2/1-ODE solution was added into the larger flask containing the metal salts and oleylamine under ambient conditions. After mixing the metal and selenium sources, one neck of the reaction flask was connected to the nitrogen flow and the reaction solution began to foam. In the meanwhile, the top of condenser was connected to a glass bottle to collect the overflowed foam. Please note that this step should be completed as soon as possible, otherwise, the generated foam would possibly spill out of the flask. Then the reaction temperature was elevated from 100 °C to 280 °C over 20 min, and this temperature was maintained for 30 min. Continuous nitrogen flow was used to remove water and oxygen during the reaction process.

When the reaction was completed, the flask was removed from the heating mantle to cool down the solution. The brown-black product was collected and centrifuged at 8000 rpm for 5 min. The upper yellow solution was discarded and the obtained nanocrystals were washed with hexane and ethanol. For TEM observations and UV–vis absorption measurements, we needed to repeat the washing procedure twice. For PXRD, ICP, and hot-pressing, the washing procedure needed to be repeated at least 5 cycles until the nanocrystals could not be dispersed in hexane any more.

To remove any organic ligands, the nanocrystals were stirred in a mixture of 85% hydrazine (CAUTION: please note that hydrazine should be handled with extreme caution due to its high toxicity) and hexane with volume ratio of 1:2 for several hours until the nanocrystals were easy to get into the hydrazine phase. Then the upper hexane phase was removed and fresh hexane was added. This process were repeated for 3 cycles. The hydrazine-capped nanocrystals were collected by centrifugation and vacuum-dried for hot-pressing. The obtained powder (about 1.8 g) was loaded into a graphite die and compacted into a dense material under a uniaxial pressure of 60 MPa in an Ar atmosphere. The hot-press temperature ranged from 450 °C to 550 °C.

Measurements: The product was characterized by powder X-ray power diffraction (XRD), using a Philips X'Pert PRO SUPER X-ray diffractometer equipped with graphite monochromatic Cu K_α radiation ($\lambda = 1.54056$ Å). The operation voltage and current were kept at 40 kV and 400 mA, respectively. TEM observations were performed on Hitachi H-7650 and JEOL-F2010 instruments with an acceleration voltage of 200 kV. The morphologies of the nanoparticles after removing the capping ligands, and the fracture of the hot-pressed pellets were characterized using field-emission scanning electron microscopy (Zeiss, Super 40). Inductively coupled plasma atomic emission spectrometry (ICP-AES) measurements were conducted using an Atomscan Advantage Spectrometer (Thermo Ash Jarrell Corporation, USA).

For the electrical conductivity and Seebeck coefficient measurements, bar samples about 1.5 mm × 1.5 mm × 10 mm in perpendicular direction (to the press direction) were measured using a commercial four-probe apparatus (ULVAC-RIKO ZEM-3). The thermal diffusivities λ in the parallel direction were obtained by the laser flash method (Netzsch LFA457) performed on round disk samples with diameters of about 12.5 mm and thicknesses of about 1 mm. The specific heat, C_p, was measured on a DSC-Q2000 instrument (TA) using sapphire as a calibration sample. The thermal conductivity was calculated from $\kappa = \lambda C_p \rho$, where ρ is the density of the sample determined by Archimedes' method.

Supporting Information

Supporting Information is available from the Wiley Online Library or from the author. The UV–vis–NIR spectrum of the nanocrystals dispersed in hexane, the XRD pattern of the hot-pressed pellets, and the calculated electron thermal conductivities are available.

Acknowledgements

We acknowledge the funding support from the National Basic Research Program of China (Grant 2010CB934700), the National Natural Science Foundation of China (Grants 91022032, 21061160492, J1030412), the Chinese Academy of Sciences (Grant KJZD-EW-M01-1), the International Science & Technology Cooperation Program of China (Grant 2010DFA41170), the Principal Investigator Award by the National Synchrotron Radiation Laboratory at the University of Science and Technology of China, and the CAS Special Grant for Postgraduate Research, Innovation and Practice.

Received: July 15, 2012
Revised: August 10, 2012
Published online: September 10, 2012

[1] a) D. Y. Chung, T. Hogan, P. Brazis, M. Rocci-Lane, C. Kannewurf, M. Bastea, C. Uher, M. G. Kanatzidis, *Science* **2000**, *287*, 1024; b) K. F. Hsu, S. Loo, F. Guo, W. Chen, J. S. Dyck, C. Uher, T. Hogan, E. K. Polychroniadis, M. G. Kanatzidis, *Science* **2004**, *303*, 818; c) B. Poudel, Q. Hao, Y. Ma, Y. C. Lan, A. Minnich, B. Yu, X. A. Yan, D. Z. Wang, A. Muto, D. Vashaee, X. Y. Chen, J. M. Liu, M. S. Dresselhaus, G. Chen, Z. F. Ren, *Science* **2008**, *320*, 634; d) A. I. Boukai, Y. Bunimovich, J. Tahir-Kheli, J. K. Yu, W. A. Goddard, J. R. Heath, *Nature* **2008**, *451*, 168; e) J. P. Heremans, V. Jovovic, E. S. Toberer, A. Saramat, K. Kurosaki, A. Charoenphakdee, S. Yamanaka, G. J. Snyder, *Science* **2008**, *321*, 554; f) J. S. Rhyee, K. H. Lee, S. M. Lee, E. Cho, S. Il Kim, E. Lee, Y. S. Kwon, J. H. Shim, G. Kotliar, *Nature* **2009**, *459*, 965.

[2] F. J. DiSalvo, *Science* **1999**, *285*, 703.

[3] a) A. J. Minnich, M. S. Dresselhaus, Z. F. Ren, G. Chen, *Energy Environ. Sci.* **2009**, *2*, 466; b) M. G. Kanatzidis, *Chem. Mater.* **2010**, *22*, 648; c) P. Pichanusakorn, P. Bandaru, *Mater. Sci. Eng. R: Rep.* **2010**, *67*, 19.

[4] Y. Ma, Q. Hao, B. Poudel, Y. C. Lan, B. Yu, D. Z. Wang, G. Chen, Z. F. Ren, *Nano Lett.* **2008**, *8*, 2580.

[5] a) X. W. Wang, H. Lee, Y. C. Lan, G. H. Zhu, G. Joshi, D. Z. Wang, J. Yang, A. J. Muto, M. Y. Tang, J. Klatsky, S. Song, M. S. Dresselhaus, G. Chen, Z. F. Ren, *Appl. Phys. Lett.* **2008**, *93*; b) G. Joshi, H. Lee, Y. C. Lan, X. W. Wang, G. H. Zhu, D. Z. Wang, R. W. Gould, D. C. Cuff, M. Y. Tang, M. S. Dresselhaus, G. Chen, Z. F. Ren, *Nano Lett.* **2008**, *8*, 4670.

[6] J. Androulakis, C. H. Lin, H. J. Kong, C. Uher, C. I. Wu, T. Hogan, B. A. Cook, T. Caillat, K. M. Paraskevopoulos, M. G. Kanatzidis, *J. Am. Chem. Soc.* **2007**, *129*, 9780.

[7] S. Johnsen, J. Q. He, J. Androulakis, V. P. Dravid, I. Todorov, D. Y. Chung, M. G. Kanatzidis, *J. Am. Chem. Soc.* **2011**, *133*, 3460.

[8] K. Biswas, H. Jiaqing, Z. Qichun, W. Guoyu, C. Uher, V. P. Dravid, M. G. Kanatzidis, *Nat. Chem.* **2011**, *3*, 160.

[9] L. D. Hicks, M. S. Dresselhaus, *Phys. Rev. B: Condens. Matter* **1993**, *47*, 12727.

[10] a) M. Scheele, N. Oeschler, K. Meier, A. Kornowski, C. Klinke, H. Weller, *Adv. Funct. Mater.* **2009**, *19*, 3476; b) M. R. Dirmyer, J. Martin, G. S. Nolas, A. Sen, J. V. Badding, *Small* **2009**, *5*, 933; c) R. J. Mehta, Y. Zhang, C. Karthik, B. Singh, R. W. Siegel, T. Borca-Tasciuc, G. Ramanath, *Nat. Mater.* **2012**, *11*, 233.

[11] a) R. J. Mehta, C. Karthik, B. Singh, R. Teki, T. Borca-Tasciuc, G. Ramanath, *ACS Nano* **2010**, *4*, 5055; b) M. Scheele, N. Oeschler, I. Veremchuk, K. G. Reinsberg, A. M. Kreuziger, A. Kornowski, J. Broekaert, C. Klinke, H. Weller, *ACS Nano* **2010**, *4*, 4283; c) Y. X. Zhao, J. S. Dyck, B. M. Hernandez, C. Burda, *J. Am. Chem. Soc.* **2010**, *132*, 4982.

[12] A. Soni, Y. Y. Zhao, L. G. Yu, M. K. K. Aik, M. S. Dresselhaus, Q. H. Xiong, *Nano Lett.* **2012**, *12*, 1203.

[13] H. R. Yang, L. A. Jauregui, G. Q. Zhang, Y. P. Chen, Y. Wu, *Nano Lett.* **2012**, *12*, 540.

[14] F. J. Fan, B. Yu, Y. X. Wang, Y. L. Zhu, X. J. Liu, S. H. Yu, Z. F. Ren, *J. Am. Chem. Soc.* **2011**, *133*, 15910.

[15] M. Ibanez, R. Zamani, A. LaLonde, D. Cadavid, W. H. Li, A. Shavel, J. Arbiol, J. R. Morante, S. Gorsse, G. J. Snyder, A. Cabot, *J. Am. Chem. Soc.* **2012**, *134*, 4060.

[16] C. Xiao, J. Xu, K. Li, J. Peng, J. L. Yang, Y. Xie, *J. Am. Chem. Soc.* **2012**, *134*, 4287.

[17] a) J. S. Son, K. Park, M. K. Han, C. Kang, S. G. Park, J. H. Kim, W. Kim, S. J. Kim, T. Hyeon, *Angew. Chem. Int. Ed.* **2011**, *50*, 1363; b) A. Shavel, D. Cadavid, M. Ibanez, A. Carrete, A. Cabot, *J. Am. Chem. Soc.* **2012**, *134*, 1438.

[18] a) M. L. Liu, F. Q. Huang, L. D. Chen, I. W. Chen, *Appl. Phys. Lett.* **2009**, *94*, 202103; b) X. Y. Shi, F. Q. Huang, M. L. Liu, L. D. Chen, *Appl. Phys. Lett.* **2009**, *94*, 122103.

[19] M.-L. Liu, I. W. Chen, F.-Q. Huang, L.-D. Chen, *Adv. Mater.* **2009**, *21*, 3808.

[20] X. Y. Shi, L. L. Xi, J. Fan, W. Q. Zhang, L. D. Chen, *Chem. Mater.* **2010**, *22*, 6029.

[21] a) M. E. Norako, R. L. Brutchey, *Chem. Mater.* **2010**, *22*, 1613; b) M. E. Norako, M. J. Greaney, R. L. Brutchey, *J. Am. Chem. Soc.* **2012**, *134*, 23; c) J. J. Wang, J. S. Hu, Y. G. Guo, L. J. Wan, *NPG Asia Mater.* **2012**, *4*, e2.

[22] a) A. Shavel, D. Cadavid, M. Ibanez, A. Carrete, A. Cabot, *J. Am. Chem. Soc.* **2012**, *134*, 1438; b) A. Shavel, J. Arbiol, A. Cabot, *J. Am. Chem. Soc.* **2010**, *132*, 4514.

[23] G. Delgado, A. Mora, G. Marcano, C. Rincón, *Mater. Res. Bull.* **2003**, *38*, 1949.